

# Finite Element Analysis of 3-Wheeler Side Bumper Beam Using Composite Material

Shubhankar R. Shende<sup>1\*</sup>, Tushar A. Jadhav<sup>2</sup>, Amar P Pandhare<sup>3</sup>

Department of Mechanical Engineering  
Sinhgad College of Engineering, Savitribai Phule Pune University, India  
\*Corresponding Author-shubhankars2002@gmail.com

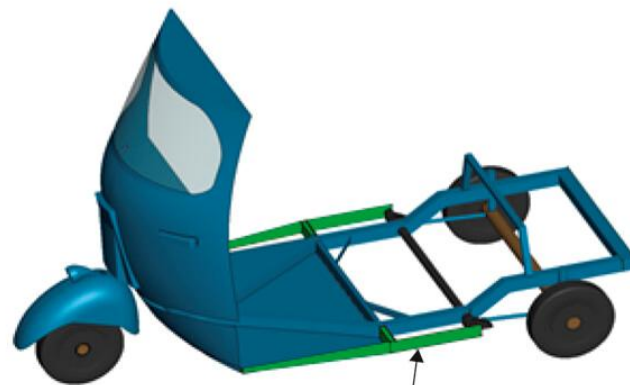
\*\*\*

**Abstract** – For the three-wheeler vehicle efficiency and safety is very much depend on the structural performance of their bumper systems, which must absorb impact energy while maintaining low weight for improved fuel economy. Even though the conventional steel bumper is structurally strong, it increases the mass of vehicle and can go under corrosion and it is permanently deformed during impact. To address these limitations, this project focuses on the design and strength optimization of a three-wheeler side bumper beam using composite materials. In this study, bumper beams of different cross-sectional geometries—such as rectangular, B-section, and hat-section—are modeled and analyzed to identify the most effective configuration in terms of impact strength, and deformation resistance. Advanced Finite Element Analysis (FEA) is used to simulate side-impact loading and evaluate key performance parameters such as stress distribution, energy absorption, and deflection characteristics. The material design incorporates glass fiber-reinforced polymer (GFRP) and carbon fiber reinforced polymer hybrid composite systems, chosen for their high specific strength, superior impact behavior, and corrosion resistance. Further, topology and strength optimization techniques are applied to refine the selected geometry, minimizing weight while maintaining structural integrity. The results of this study are expected to reveal the most efficient cross-sectional design and composite configuration suitable for side bumper beams in three-wheelers. Overall, the project contributes to the development of high performance, safe, and sustainable automotive structures, offering a viable alternative to conventional metallic designs for improved vehicle safety and performance.

**Key Words:** Bumper beam, epoxy, glass fiber, carbon fiber, mechanical properties, reinforced composite, energy absorption, crashworthiness.

## 1. INTRODUCTION

Three-wheelers are widely used in urban transport especially in developing countries, where they are used as low-cost passenger and cargo carriers. However, their light construction and narrow track width make them very vulnerable to side-impact collisions. The lack of strong side structures can lead to excessive intrusion and inadequate energy absorption in side impact collisions, presenting a major safety hazard to occupants. To overcome this challenge, the design of a high-performance side bumper beam is required to improve the structural integrity and crash protection of such vehicles.



Side bumper beam

With the rapid development of the composite material industry in recent years, the development of excellent performance composite materials to replace traditional materials has become the important direction for the development of lightweight vehicles. In case of hybrid beam found by Shada B [1] in the study, the use of the composite material can increase the impact energy absorption by 75%. Bing Du's study [2] indicates that the cost of investment on the study of composite materials is relatively high in the initial stage, but it will decrease with the improvement and maturity of the process. Furthermore, the application of composite materials in automobile lightweight will be additionally extensive after that. In the impact test, the composite bumper beam has better impact resistance and higher class of lightweight than that of steel. The study by Tshilidzi M. [3] reviews the evolution of materials, design optimization methods, manufacturing advancements, and crashworthiness requirements of modern automotive bumper beams in the era of the Fourth Industrial Revolution (4IR). It also highlights the increasing importance of smart bumper systems and AI-driven technologies in improving future vehicle safety and performance. Vinjavarapu S. [4] has studied on the effect of glass, jute and rami fibers on mechanical properties of composite materials. The results indicated that the mechanical performance of the composite was strongly dependent on the composition and arrangement of the reinforcement materials. The best alternative to conventional plastics was found to be the Glass-Rami-Rami-Jute-Jute-Glass pattern among the various configurations tested. Similarly, the research of Yeshanew, E. S., et al. [5] revealed that carbon polyamide bumper has better energy absorption ability than traditional steel and aluminum bumpers by 11.15% and 16.3%, respectively. In addition, the carbon polyamide bumper reduced the total weight by 9.7 kg, nearly 47.5% lighter than the steel bumper.

This research focuses on the design and strength optimization of a three-wheeler side bumper beam using composite materials, checking different cross-sectional configurations to identify the most effective combination of stiffness, strength, and energy absorption. Using advanced CAD modeling and finite element analysis, various composite layouts and

geometries are evaluated under simulated impact conditions. The outcomes aim to support the development of safer, lighter, and more durable side protection structures for three-wheelers, contributing to enhanced occupant safety and overall vehicle performance

## 2. THE BUMPER BEAM AND IT'S IMPORTANCE

The bumper beam is a critical component of the vehicle and is designed to absorb the energy of impact in collisions and to protect other vehicle components from damage. It is located in the front and rear of the vehicle. The primary purpose of it is to effectively absorb and dissipate the energy generated by an impact. During a collision, the bumper beam helps in reducing the force transmitted to the chassis, thereby minimizing structural damage and enhancing passenger safety. To perform this function efficiently, the bumper beam must have a high impact strength to absorb energy and a high Young's modulus to retain stiffness, structural strength and shape after a collision. Traditionally, bumper beams have been made from aluminium and high-strength steel.

However, the increasing demand for lightweight vehicles and improved fuel efficiency has led to the extensive use of advanced materials such as plastics and composite materials for the manufacture of bumper beams.

In engineering practice, the bumper beam design needs a careful choice of material, the cross-sectional geometry and energy absorption characteristics. Historically, metals like steel and aluminum have been employed because of their strength and durability. However, the need for lightweight vehicles and better fuel economy is increasing the use of composite materials. Composite bumper beams have attractive features like high strength-to-weight ratio, corrosion resistance and the ability to tailor material properties by controlling fiber orientation and layering. These features make them highly appropriate for absorbing impact energy and reducing the total weight of the vehicle, which directly helps to improve performance and efficiency.

In many cases, the side structure of a 3-wheeler offers minimal protection to passengers, especially in the event of lateral collisions. Therefore, the introduction of a side bumper beam is crucial to enhance side-impact protection by absorbing and redistributing the impact energy away from the passenger cabin.

## 3 FEA OF THREE-WHEELER SIDE BUMPER BEAM

For a 3-wheeler side bumper beam, the design should aim to achieve maximum energy absorption while adding as little weight as possible, since extra weight can negatively affect the vehicle's stability, fuel efficiency, and maneuverability. The bumper beam must be strong enough to withstand low to moderate impact loads that are common in urban traffic conditions, including collisions with other vehicles, poles, or roadside obstacles. Composite materials are highly suitable for this application because they can be designed to undergo progressive failure and controlled deformation, which helps in absorbing and dissipating impact energy more effectively. In addition, the cross-sectional geometry of the side bumper beam, such as tubular, B-section, or hat-type designs, has a significant influence on its stiffness, strength, and overall crashworthiness performance.

### 3.1 GEOMETRIC MODELING OF SIDE BUMPER BEAM CROSS-SECTIONS:

The present work focuses on the Finite Element analysis a three-wheeler side bumper beam using composite materials to design and strength optimization of existing cross-sectional

area used in current market. The methodology adopted follows a systematic engineering approach involving baseline study, conceptual design, finite element analysis, and optimization. Three different cross-sectional configurations—Hat section, B-section, and rectangular section—are considered to evaluate their structural performance under identical loading and boundary conditions.

A baseline model of the existing steel bumper beam is first analyzed to establish reference performance parameters such as stiffness, strength, deformation, and energy absorption. This baseline serves as a benchmark against which all proposed composite designs are evaluated. The use of a baseline model is essential to quantify improvements and validate the effectiveness of the new design. The dimensions for the models are taken from considering the space and the current side bumper beam. Length is same for the selected cross sections i.e. 1600mm. Following the baseline study, multiple design concepts are generated based on different cross-sectional geometries, namely Hat section, B-section, and rectangular section. Following figure 1 shows the different cross section taken into account for the study.

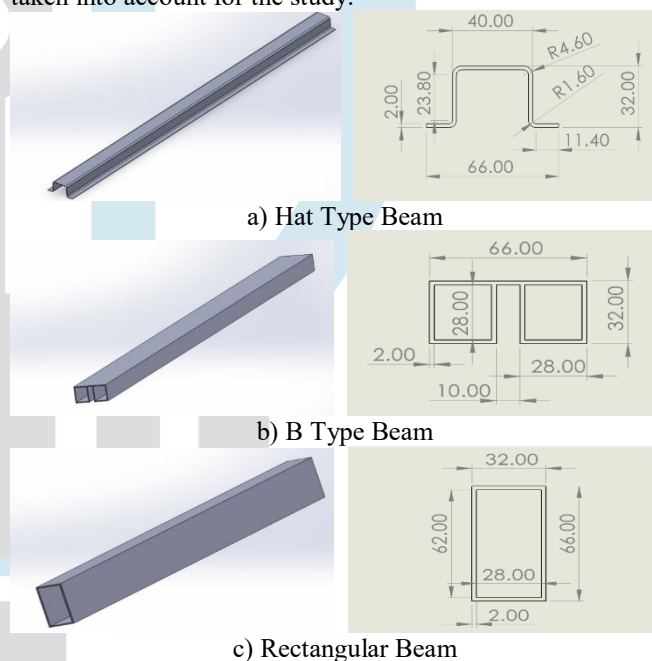


Fig - 1 Cross section of side bumper beam for study

Each cross-section has unique advantages in terms of load distribution, bending resistance, and manufacturability. Initially all the cross sections are analyzed by considering the material as steel, which is widely used in industry. By analyzing these configurations under identical conditions, a comparative understanding of their performance is achieved.

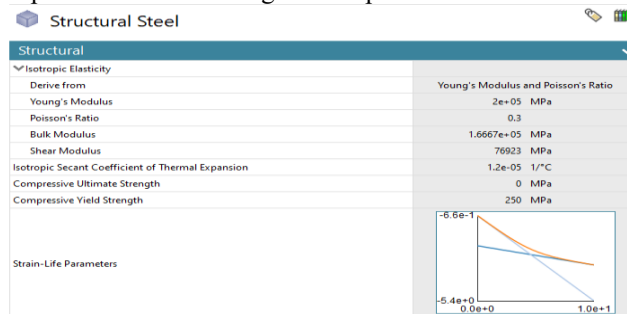


Fig - 2 Material Properties of Structural Steel.

### 3.2 EXPLICIT DYNAMIC ANALYSIS OF CROSS SECTION:

#### 1. Hat -Type Side Bumper Beam: -

Following figure represents CAD arrangement of beam for the side impact in ANSYS software. Two rollers at bottom acts as

fixed support and the one roller above the beam has velocity of 8333.3 mm/s.

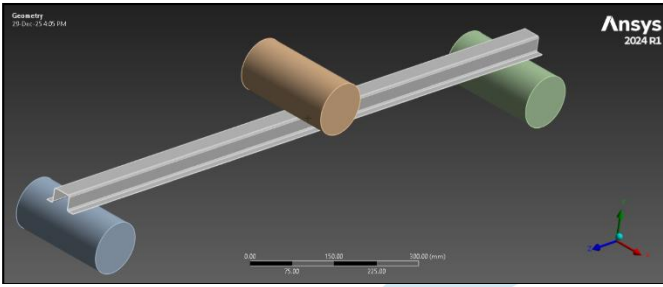


Fig – 2 CAD arrangement for explicit dynamic analysis

Below figure 3 shows finite mesh model of hat type beam contains 19579 nodes and 16050 elements and the size of element is 10 mm.

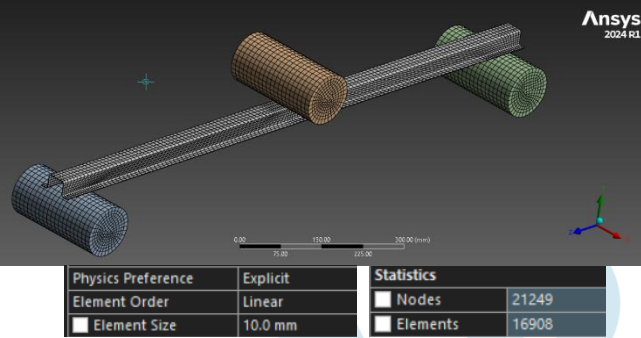


Fig - 3 Mesh model of Hat-type side bumper beam

Boundary conditions are then applied as shown in below Fig. 4, blue color represents fixed support and the yellow one has velocity applied to it in downward Y direction.

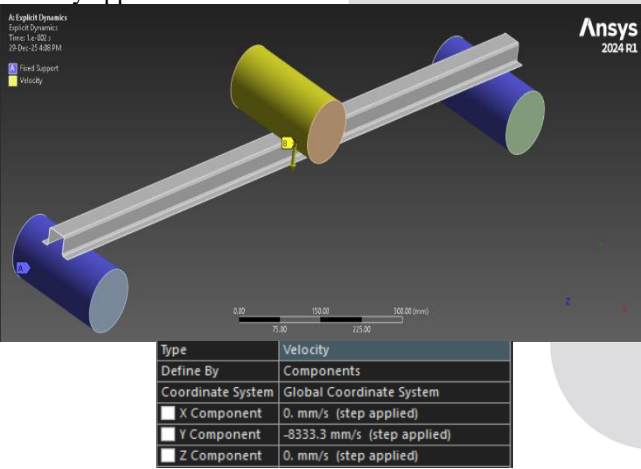
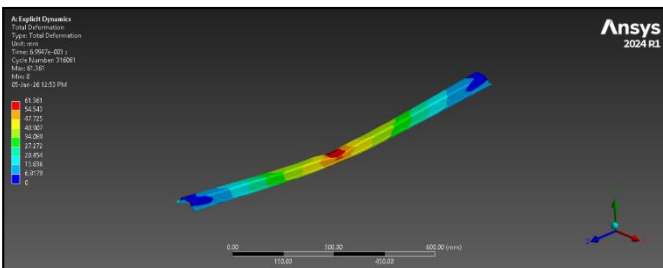
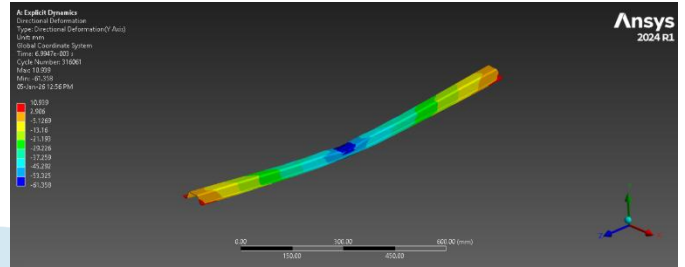


Fig - 4 Boundary condition of Hat-type side bumper beam

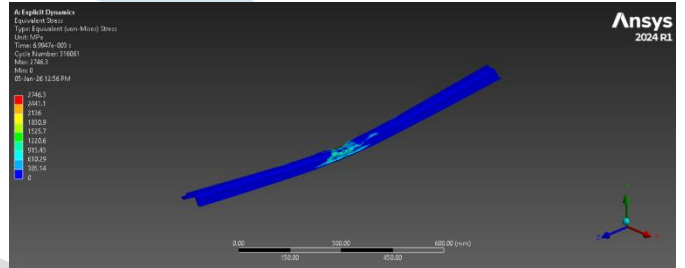
After the meshing and assigning the correct boundary condition material and other factors such as velocity type of contact etc. the results are calculated in ANSYS software. Results such as total deformation, directional deformation equivalent stress, force reaction and energy absorption are calculated. Below are the results for Hat type beam from ANSYS in explicit dynamic conditions.



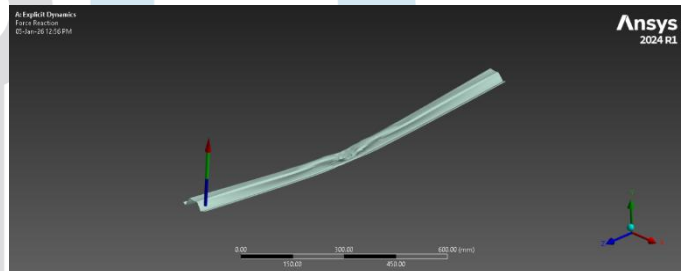
a) Total deformation of Hat-type side bumper beam is 61.361 mm



b) Directional deformation of Hat-type side bumper beam is 61.158 mm



c) Equivalent stress of Hat-type side bumper beam is 2746.3 N



d) Force reaction of Hat-type side bumper beam.

Fig - 5 Results of Hat-type side bumper beam

Time Vs Internal Energy graph is showed in following figure 6 for Hat Type Beam. As the time passes internal energy of beam is increased which shows that beam has absorbed the impact energy. At the time of impact around 250 J of energy is absorbed by beam with the deflection of 61 mm Approx.

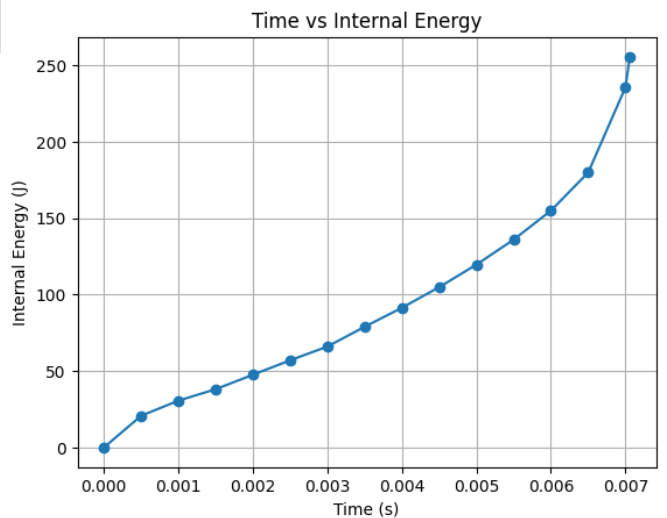


Fig - 6 Time vs Internal Energy

2. B-Type Side Bumper Beam: -

Following figure represents CAD arrangement of beam for the side impact in ANSYS software. Two rollers at bottom acts as

fixed support and the one roller above the beam has velocity of 8333.3 mm/s.

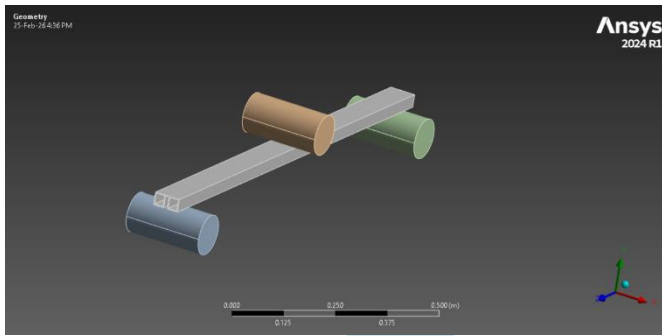


Fig – 7 CAD arrangement for explicit dynamic analysis

Mesh is created with element size of 10mm and nodes and elements generated are 25068 and 19348 respectively show in figure 8.

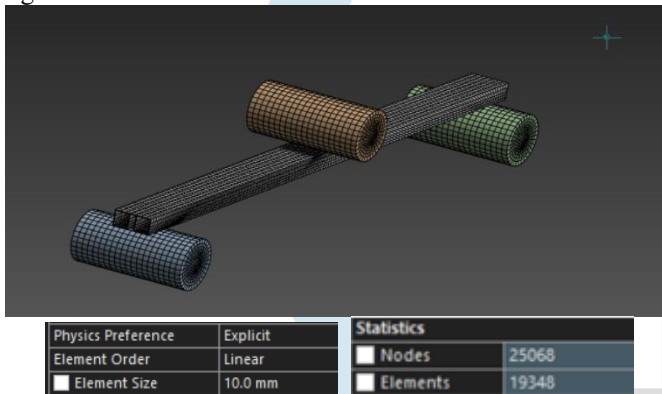


Fig - 8 Mesh model of B-type side bumper beam

Boundary conditions are then applied as shown in below Fig. 4, blue color represents fixed support and the yellow one has velocity applied to it in downward Y direction.

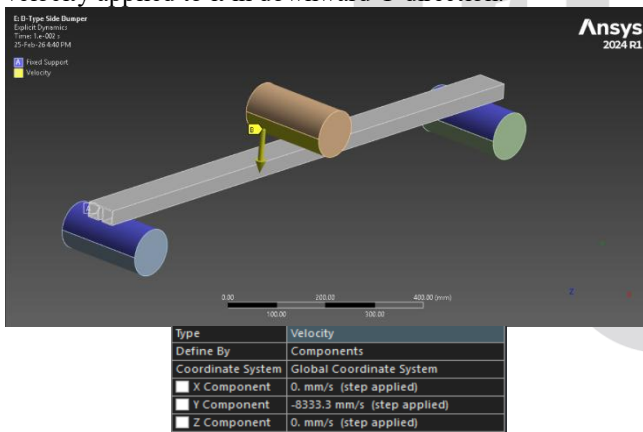
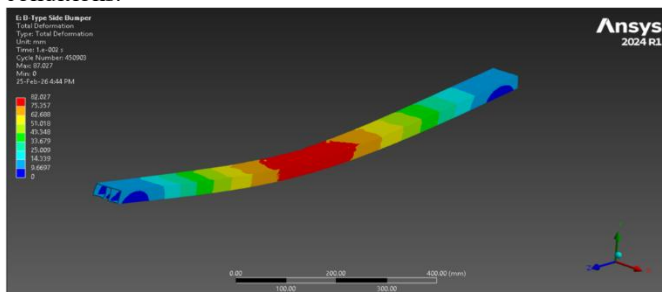
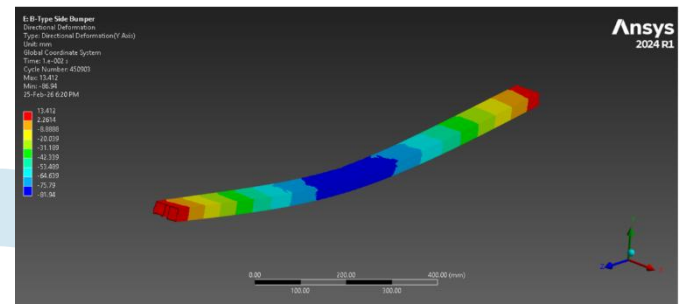


Fig - 9 Boundary condition of B-type side bumper beam

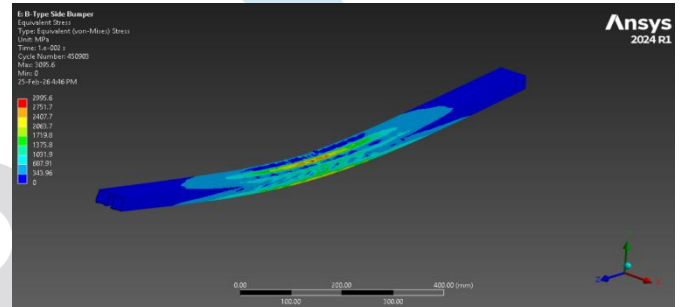
After the meshing and assigning the correct boundary condition material and other factors such as velocity type of contact etc. the results are calculated in ANSYS software. Results such as total deformation, directional deformation equivalent stress, force reaction and energy absorption are calculated. Below are the results for B type beam from ANSYS in explicit dynamic conditions.



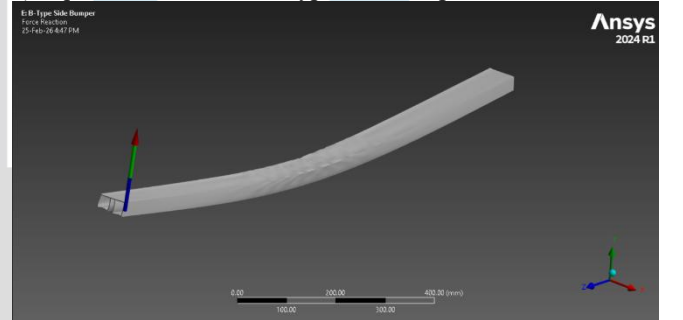
a) Total deformation of B-type side bumper beam is 87.027 mm



b) Direction deformation of B -type side bumper beam is 81.94 mm



c) Equivalent stress of B-type side bumper beam is 2995.6 N



| Maximum Value Over Time                   |          |
|---|----------|
| <input type="checkbox"/> X Axis           | 2549.6 N |
| <input type="checkbox"/> Y Axis           | 12533 N  |
| <input type="checkbox"/> Z Axis           | 1149.9 N |
| <input checked="" type="checkbox"/> Total | 12738 N  |

d) Force reaction of B-type side bumper beam.

Fig - 10 Results of B-type side bumper beam

Time Vs Internal Energy graph is showed in following figure 11 for B Type Beam. As the time passes internal energy of beam is increased which shows that beam has absorbed the impact energy. At the time of impact above 750 J of energy is absorbed by beam with the defection of 81.94 mm Approx.

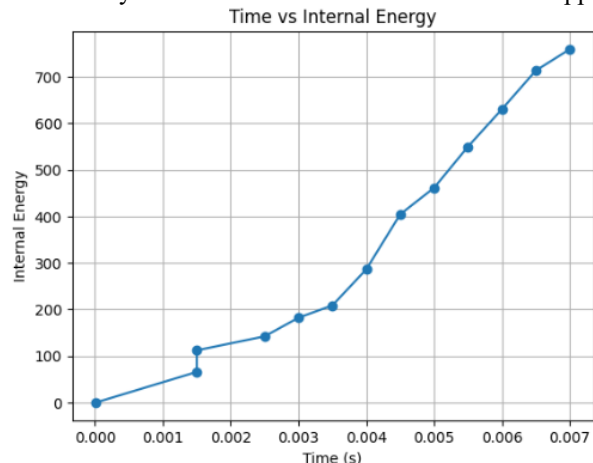


Fig - 11 Time vs Internal Energy

3. Rectangular-Type Side Bumper Beam: -

Following figure represents CAD arrangement of beam for the side impact in ANSYS software. Two rollers at bottom acts as fixed support and the one roller above the beam has velocity of 8333.3 mm/s.

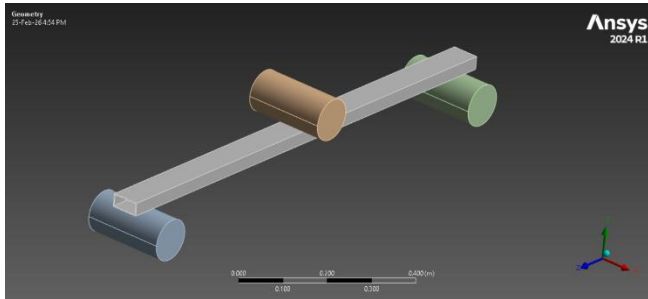
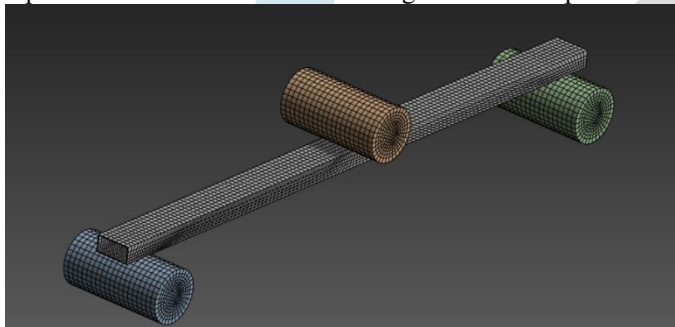


Fig – 12 CAD arrangement for explicit dynamic analysis

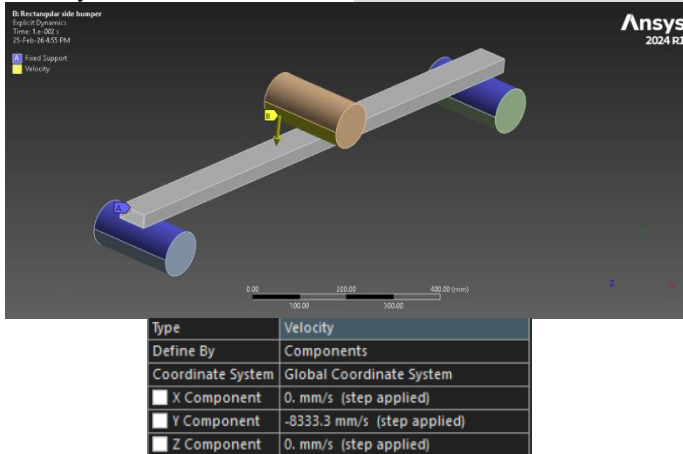
For the Rectangular type beam quadrilateral and hexahedral mesh is created such that there are 23334 nodes and 17598 elements created with element size of 10mm. Figure 13 represents the mesh model of rectangular side bumper beam.



| Physics Preference |         | Statistics |       |
|--------------------|---------|------------|-------|
| Element Order      | Linear  | Nodes      | 23334 |
| Element Size       | 10.0 mm | Elements   | 17598 |

Fig - 13 Mesh model of Rectangular-type side bumper beam

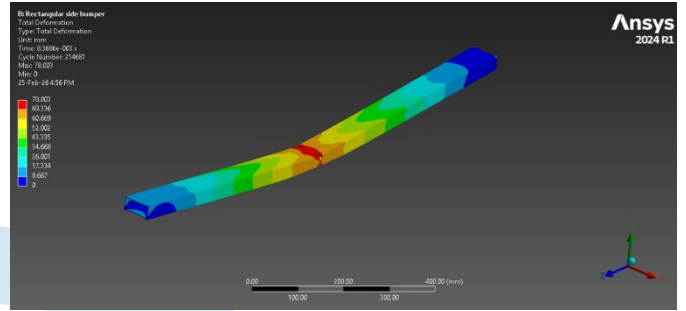
Boundary conditions are applied to model with two rollers as fixed supports beam resting on them and one roller with velocity of 8333.3 mm/sec in downward Y direction.



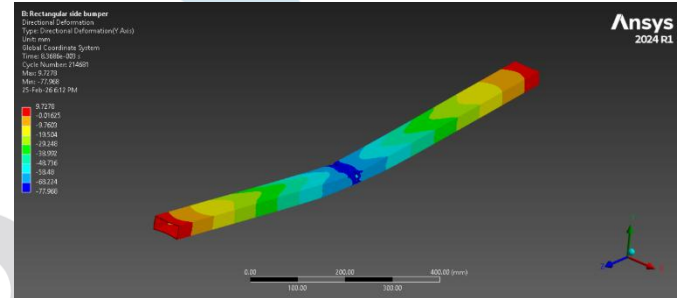
| Type              | Velocity                    |
|-------------------|-----------------------------|
| Define By         | Components                  |
| Coordinate System | Global Coordinate System    |
| X Component       | 0. mm/s (step applied)      |
| Y Component       | -8333.3 mm/s (step applied) |
| Z Component       | 0. mm/s (step applied)      |

Fig - 14 Boundary condition of Rectangular -type side bumper beam

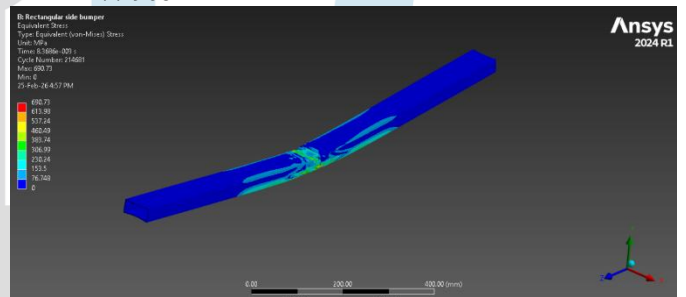
After the meshing and assigning the correct boundary condition material and other factors such as velocity type of contact etc. the results are calculated in ANSYS software. Results such as total deformation, directional deformation equivalent stress, force reaction and energy absorption are calculated. Below are the results for rectangular type beam from ANSYS in explicit dynamic conditions.



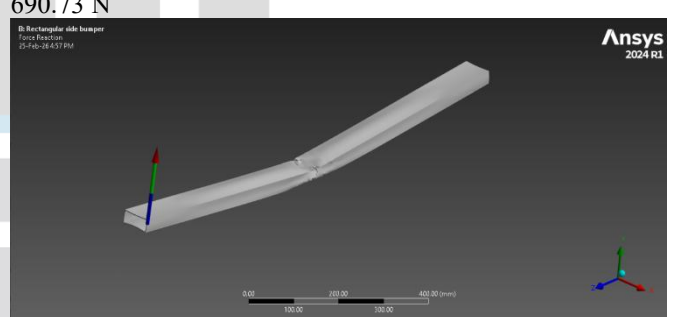
a) Total deformation of Rectangular-type side bumper beam is 78.003 mm



b) Directional deformation of Rectangular-type side bumper beam is 77.968 mm



c) Equivalent stress of Rectangular-type side bumper beam is 690.73 N



| Maximum Value Over Time |          |
|-------------------------|----------|
| X Axis                  | 790.3 N  |
| Y Axis                  | 5171.1 N |
| Z Axis                  | 366.63 N |
| Total                   | 5244. N  |

d) Force reaction of Rectangular-type side bumper beam.

Fig - 15 Results of Rectangular-type side bumper beam

Time Vs Internal Energy graph is showed in following figure 16 for Rectangular Type Beam. As the time passes internal energy of beam is increased which shows that beam has absorbed the impact energy. At the time of impact near about 300 J of energy is absorbed by beam with the deflection of 87.97 mm Approx.

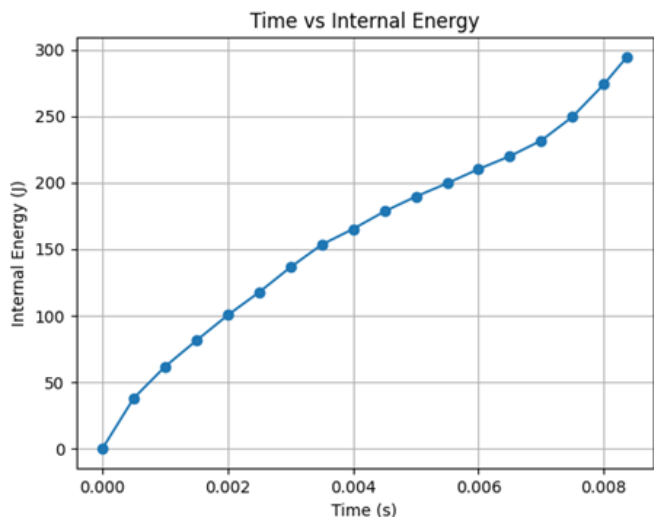


Fig - 16 Time vs Internal Energy

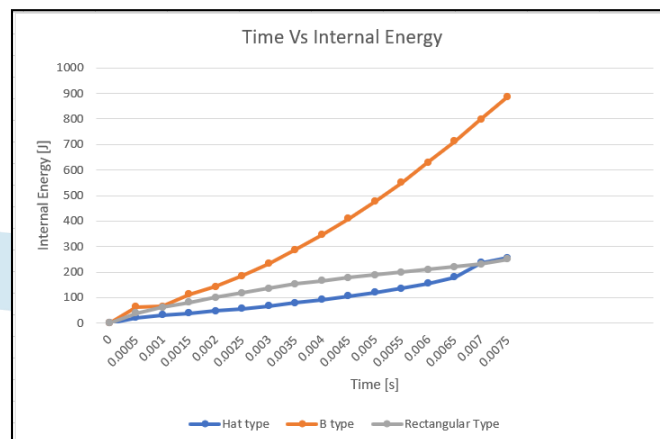


Fig - 17 Time vs Internal Energy Of different cross section

3.3 COMPARISON OF FEA RESULTS OF DIFFERENT CROSS SECTIONS: -

Table -1: Comparison of different Cross sections Ansys results

| Sr. No. | Cross Section of Beam | Total Deformation (mm) | Max Directional Deformation (mm) | Equivalent stress (Mpa or N) | Force reaction Y axis (N) | Max Internal Energy (J) |
|---------|-----------------------|------------------------|----------------------------------|------------------------------|---------------------------|-------------------------|
| 1       | Hat Type              | 61.361                 | 61.358                           | 2746.3                       | 8999.8                    | 255.58                  |
| 2       | B Type                | 82.027                 | 81.94                            | 2995.6                       | 12533                     | 886.84                  |
| 3       | Rectangular Type      | 78.003                 | 77.968                           | 690.73                       | 5171.1                    | 294.49                  |

Finite Element Analysis (FEA) was initially carried out on three different cross-sectional geometries of the side bumper beam, namely Hat-type, B-type, and rectangular sections, under identical loading and boundary conditions to identify the most suitable structural configuration.

For the Hat-type geometry, the maximum total deformation obtained was 61.361 mm, while the maximum directional deformation was 61.358 mm. The maximum equivalent (von Mises) stress reached 2746.3 MPa, and the structure generated a maximum reaction force of 8999.8 N. The total energy absorbed by this geometry during loading was 255.58 J.

For the B-type geometry, the maximum total deformation was 82.027 mm, and the maximum directional deformation was 81.94 mm. The equivalent stress developed in the beam reached 2995.6 MPa. However, this configuration demonstrated the highest load-carrying capability among the three geometries with a maximum reaction force of 12533 N and a significantly higher energy absorption of 886.84

For the Rectangular geometry, the maximum total deformation recorded was 78.003 mm, with a directional deformation of 77.968 mm. The maximum equivalent stress was 690.73 MPa, which is comparatively lower than the other geometries. The maximum reaction force was 5171.1 N, and the total energy absorbed during impact was 294.49 J.

Based on these results shown in Table 1 and Fig. 17, the B-type geometry demonstrated superior energy absorption and load resistance, indicating better crashworthiness performance. Therefore, this geometry was selected for further structural enhancement through composite reinforcement.

Further explicit dynamic analysis is carried out to check the performance of beam after reinforcement of the composite material on the beam. Epoxy carbon UD and Glass Fiber composite material reinforcement is carried out in FEA Ansys software to improve performance of B-type beam further with the help of composite material. The results are compared with the standard structural steel beam and checked the energy absorption, deflection and the reaction force.

3.4 EXPLICIT DYNAMIC ANALYSIS OF COMPOSITE MATERIAL REINFORCED BEAM

The use of composite materials in the side bumper beam of a three-wheeler plays a critical role in improving safety, performance, and overall vehicle efficiency. Traditionally, bumper beams were manufactured using metals such as steel or aluminium, but the shift toward composite materials—such as glass fiber reinforced polymers (GFRP) and carbon fiber reinforced polymers (CFRP)—has introduced several significant advantages.

In summary, the significance of composite materials in the side bumper beam of a three-wheeler lies in their ability to provide superior energy absorption, reduced weight, corrosion resistance, design flexibility, improved safety, and long-term economic and environmental benefits. These advantages make composites a highly suitable and increasingly preferred choice for modern automotive structural components.

For analysis purpose a layer of composite material is created over the B type side bumper beam in CAD model. Two different beams with different composite material are created in CAD and tested using ANSYS software. Both epoxy carbon fiber reinforced and glass fiber reinforced B type beams are analyzed.

1. Explicit Dynamic Analysis of Carbon Fiber Reinforced B-Type Side Bumper Beam: -

Following figure represents CAD arrangement of beam for the side impact in ANSYS software. Two rollers at bottom acts as fixed support and the one roller above the beam has velocity of 8333.3 mm/s.

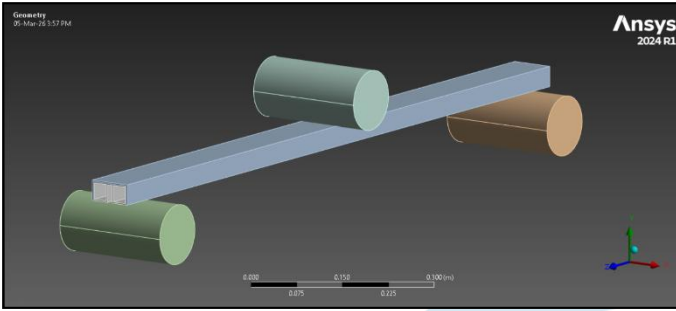


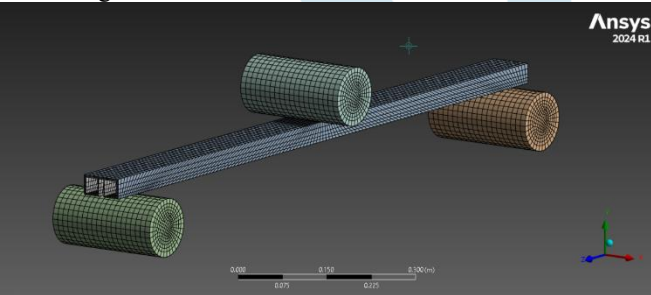
Fig – 18 CAD arrangement for explicit dynamic analysis

**Epoxy Carbon UD (230 GPa) Prepreg**  
 Typical uni-directional carbon prepreg with 230 GPa fibers (Vf=0.52)

|                             |                        |
|-----------------------------|------------------------|
| Density                     | 1490 kg/m <sup>3</sup> |
| <b>Structural</b>           |                        |
| Orthotropic Elasticity      |                        |
| Young's Modulus X direction | 1.21e+11 Pa            |
| Young's Modulus Y direction | 8.6e+09 Pa             |
| Young's Modulus Z direction | 8.6e+09 Pa             |
| Poisson's Ratio XY          | 0.27                   |
| Poisson's Ratio YZ          | 0.4                    |
| Poisson's Ratio XZ          | 0.27                   |
| Shear Modulus XY            | 4.7e+09 Pa             |
| Shear Modulus YZ            | 3.1e+09 Pa             |
| Shear Modulus XZ            | 4.7e+09 Pa             |

Fig – 19 Material Properties of Epoxy Carbon UD

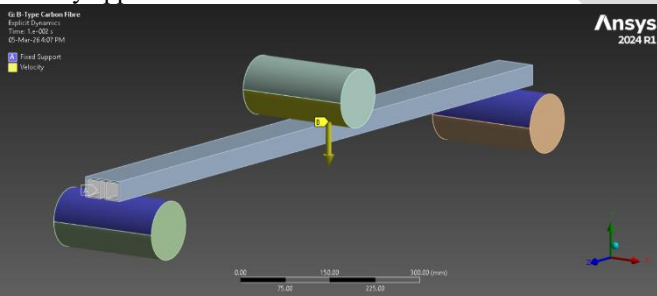
Mesh is generated in the software having quadrilateral and hexahedral mesh combination with 10 mm element size containing Nodes 30360 and elements 21924.



|                    |          |            |       |
|--------------------|----------|------------|-------|
| Physics Preference | Explicit | Statistics |       |
| Element Order      | Linear   | Nodes      | 30360 |
| Element Size       | 10.0 mm  | Elements   | 21924 |

Fig - 19 Mesh model of B-type side bumper beam

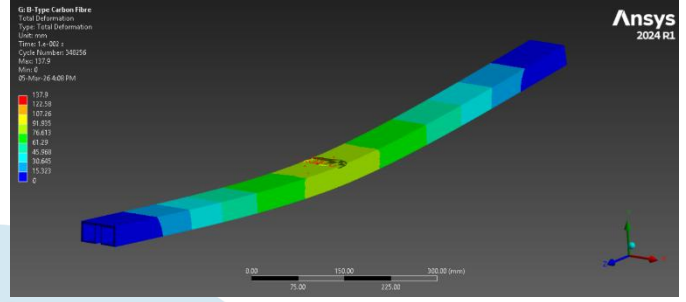
Boundary conditions are then applied as shown in below Fig. 20, blue color represents fixed support and the yellow one has velocity applied to it in downward Y direction.



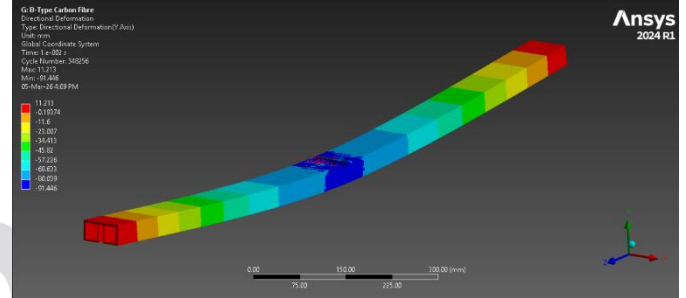
|                   |                             |
|-------------------|-----------------------------|
| Type              | Velocity                    |
| Define By         | Components                  |
| Coordinate System | Global Coordinate System    |
| X Component       | 0. mm/s (step applied)      |
| Y Component       | -8333.3 mm/s (step applied) |
| Z Component       | 0. mm/s (step applied)      |

Fig - 20 Boundary condition of B-type side bumper beam

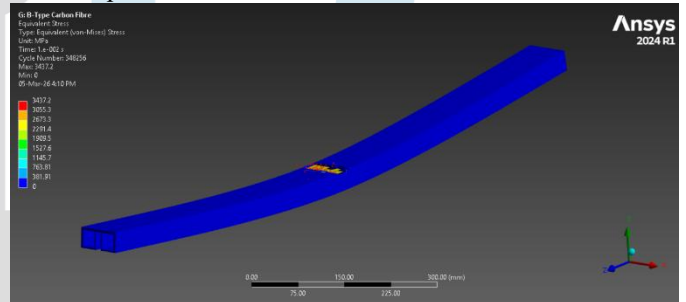
After the meshing and assigning the correct boundary condition material and other factors such as velocity type of contact etc. the results are calculated in ANSYS software. Results such as total deformation, directional deformation equivalent stress, force reaction and energy absorption are calculated. Below are the results for B type beam from ANSYS in explicit dynamic conditions.



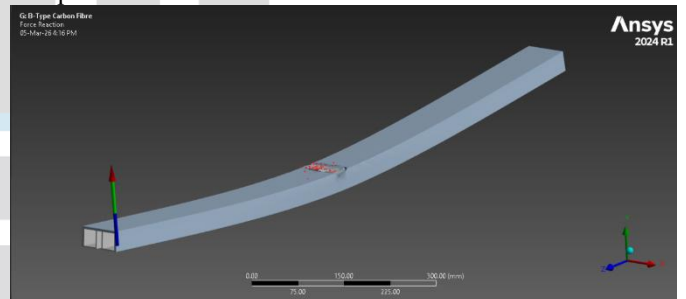
a) Total deformation of carbon fiber reinforced B-type side bumper beam



b) Directional deformation of carbon fiber reinforced B-type side bumper beam



c) Equivalent stress of carbon fiber reinforced B-type side bumper beam



| Maximum Value Over Time |          |
|-------------------------|----------|
| X Axis                  | 1641.2 N |
| Y Axis                  | 67380 N  |
| Z Axis                  | 2494.5 N |
| Total                   | 67401 N  |

d) Force reaction of B-type side bumper beam.

Fig - 21 Results of carbon fiber reinforced B-type side bumper beam

Fig 22 shows as time increased internal energy of beam is also increased which tells that beam has absorbed the impact energy which is above 900 J. This show that energy absorption of the beam has increased which shows that beam has improved crash worthiness. As the epoxy carbon UD has improved the energy absorption by 15%. The Fig 21 (c) shows that the Carbon Fiber UD layer is broken at the impact, which indicates that the material will not sustain the impact in this case.

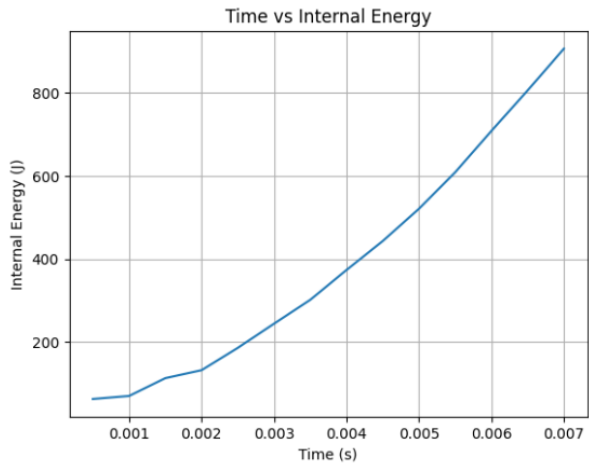


Fig - 20 Time vs Internal Energy

2. Explicit Dynamic Analysis of Glass Fiber Reinforced B-Type Side Bumper Beam

Following figure represents CAD arrangement of beam for the side impact in ANSYS software. Two rollers at bottom acts as fixed support and the one roller above the beam has velocity of 8333.3 mm/s.

Boundary conditions are then applied as shown in below Fig. 24, blue color represents fixed support and the yellow one has velocity applied to it in downward Y direction.

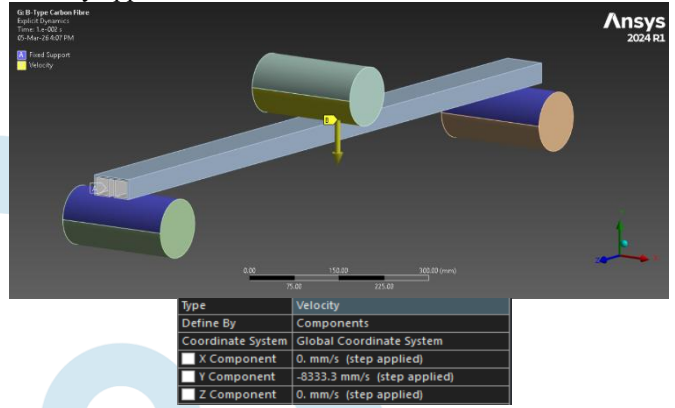


Fig - 24 Boundary condition of glass fibers reinforced B-type side bumper beam

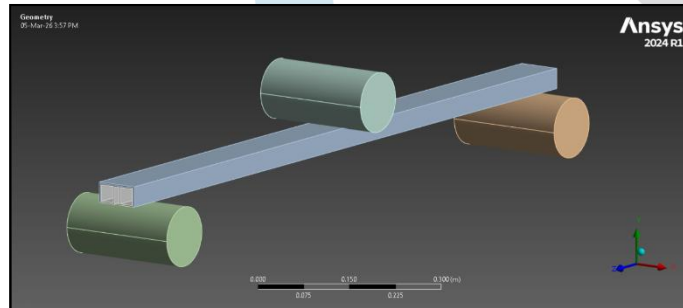


Fig - 21 CAD arrangement for explicit dynamic analysis

| E-Glass   |                                     |
|---|-------------------------------------|
| E-Glass fibers only                               |                                     |
| Density   | 2600 kg/m <sup>3</sup>              |
| <b>Structural</b>                                 |                                     |
| Isotropic Elasticity                              |                                     |
| Derive from                                       | Young's Modulus and Poisson's Ratio |
| Young's Modulus                                   | 7.3e+10 Pa                          |
| Poisson's Ratio                                   | 0.22                                |
| Bulk Modulus                                      | 4.3452e+10 Pa                       |
| Shear Modulus                                     | 2.9918e+10 Pa                       |
| Isotropic Secant Coefficient of Thermal Expansion | 5e-06 1/°C                          |
| <b>Thermal</b>                                    |                                     |
| Isotropic Thermal Conductivity                    | 1.27 W/m·°C                         |
| Specific Heat Constant Pressure                   | 802 J/kg·°C                         |

Fig - 22 Material Properties of epoxy glass fibers

Mesh is generated in the software having quadrilateral and hexahedral mesh combination with 10 mm element size containing Nodes 30360 and elements 21924.

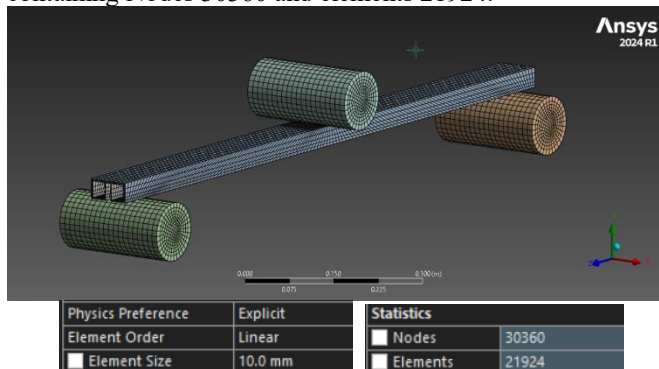
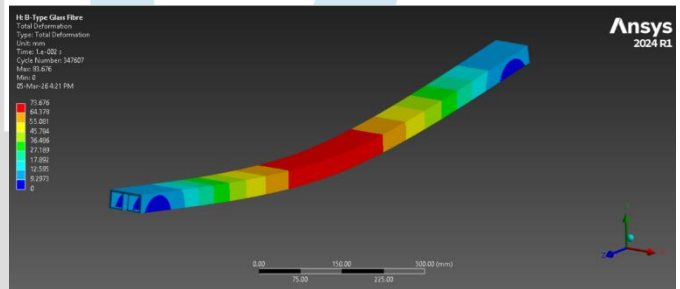
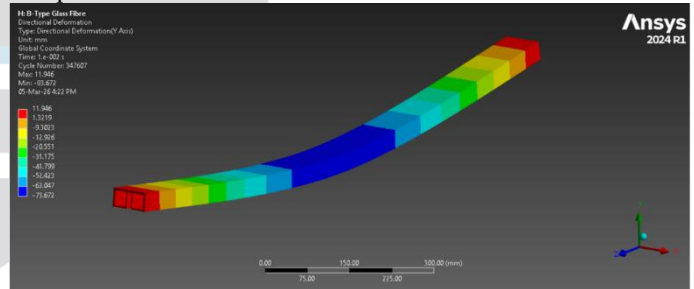


Fig - 23 Mesh model of glass fibers reinforced B-type side bumper beam

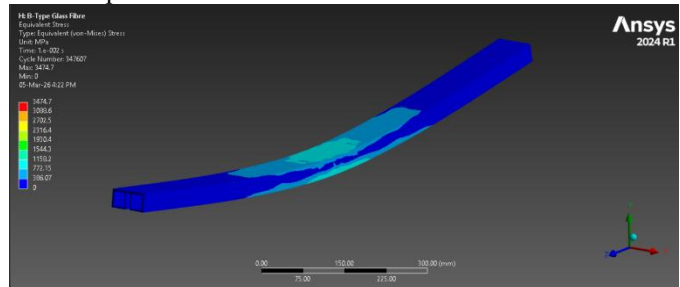
After the meshing and assigning the correct boundary condition material and other factors such as velocity type of contact etc. the results are calculated in ANSYS software. Results such as total deformation, directional deformation equivalent stress, force reaction and energy absorption are calculated. Below are the results for B type beam from ANSYS in explicit dynamic conditions.



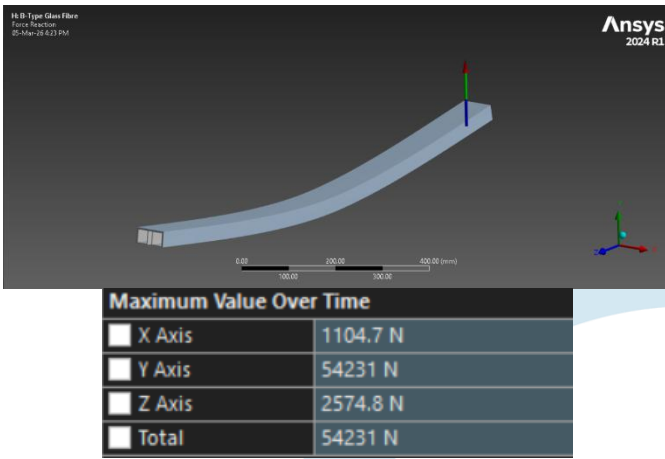
a) Total deformation of glass fibers reinforced B-type side bumper beam



b) Direction deformation of glass fibers reinforced B-type side bumper beam



c) Equivalent stress of glass fibers reinforced B-type side bumper beam



d) Force reaction of glass fibers reinforced B-type side bumper beam.

**Fig - 25** Results of glass fibers reinforced B-type side bumper beam

Fig 26 shows as time increased internal energy of beam is also increased which tells that beam has absorbed the impact energy which is above 1200 J. This show that energy absorption of the beam has increased which shows that beam has improved crash worthiness. As the Glass Fiber has improved the energy absorption by 45%.

The deformation is reduced by 12.35% in B type glass fiber reinforced beam than the conventional B type beam

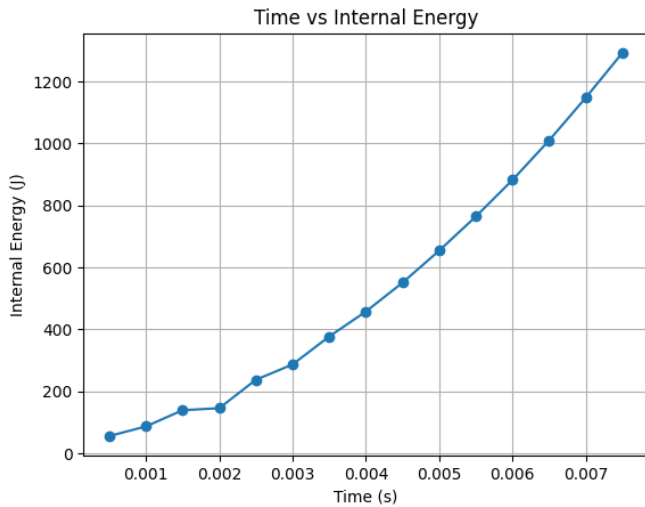


**Fig - 26** Time vs Internal Energy

#### 4. EXPERIMENTAL ANALYSIS OF SIDE BUMPER

##### 4.1 MANUFACTURING OF TEST SPECIMEN:

The fabrication of the proposed b-type side bumper beam was carried out using a hybrid approach combining metal forming and composite reinforcement techniques. Initially, a metal sheet was selected with the required thickness. The required geometry was obtained by performing a sheet metal bending operation using a press brake. Appropriate dies were used to accurately form the B-type cross-section, ensuring dimensional consistency and minimal defects such as wrinkling or spring-back.



**Fig – 27** Glass Fiber Reinforcement Preparation

Subsequently, glass fiber reinforcement was applied using a hand lay-up process. Layers of glass fiber mat were placed over the formed metal section and impregnated with a resin solution (typically epoxy or polyester).

The laminated structure was then allowed to cure at room temperature under controlled conditions to achieve sufficient bonding strength. After curing, the component was trimmed and finished to obtain the final reinforced side bumper beam.



**Fig - 28** Glass Fiber Reinforced Beam

##### 4.2 EXPERIMENTAL TESTING:

The performance of the fabricated side bumper beam was evaluated through a flexural test conducted on a Universal Testing Machine. The test was carried out using a three-point bending setup, where the specimen was supported at two ends and load was applied at the midpoint through a loading nose. Proper alignment of the specimen was ensured to avoid any eccentric loading and to obtain accurate results.



Fig – 29 Experimental Setup On UTM

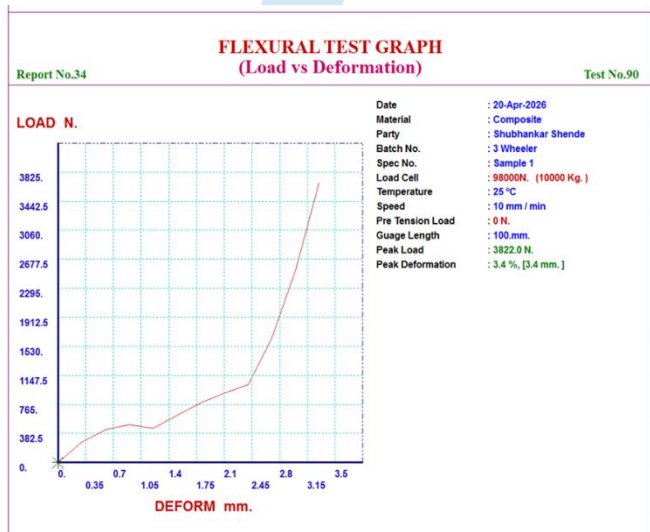


Fig – 30 Load Vs Deformation Graph on UTM

When the force applied on UTM is 3.82 KN the deformation of 3.2 mm is observed in the B type beam. Above figure 4.2.2 shows the representation of the graph of the load vs deformation on UTM.

## 5. RESULTS AND DISCUSSION

### 5.1 FEA OF EXPERIMENTAL SPECIMEN IN ANSYS:

Finite Element Analysis is carried out for the test specimen by modelling the actual test specimen in CAD. FEA is carried out by keeping all the conditions same as the experimental setup. Static three-point bending analysis is performed to validate the results of the experimental test.

By Doing this comparison of the sample specimen results in FEA and experiment we can validate the FEA results of actual B type beam came in Ansys. This validation can tell that the FEA results are close to the real-life result or not. Fig 31 represents the arrangement on UTM of the beam.

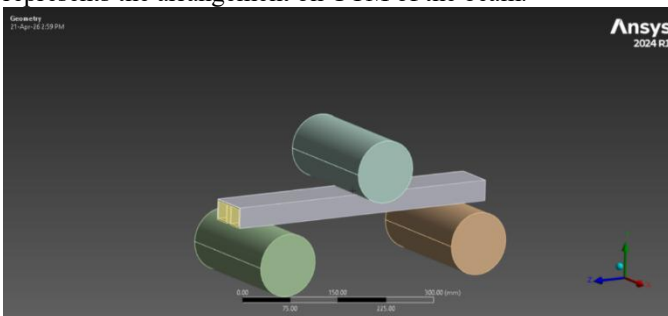


Fig - 31 Geometry of the experimental prototype.

Meshing is created with the element size of 10 mm and the numbers of elements and nodes are generated are 16576 & 20976 respectively as shown in below Fig 32

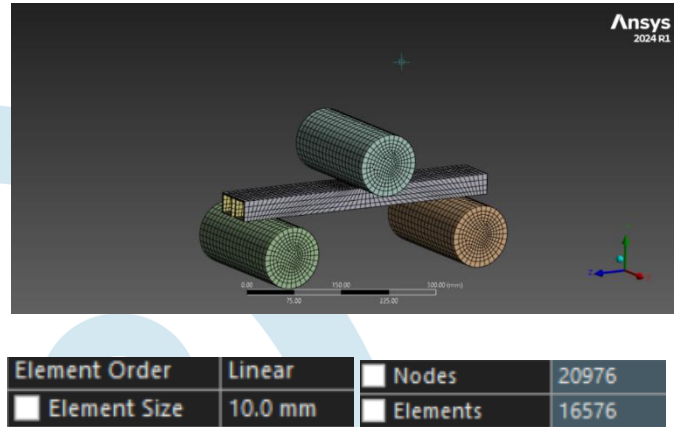


Fig - 32 Meshing Details

Boundary conditions are applied such that two rollers below are fixed supports and the one above beam is applying the force of 3822 N as shown in below Fig 33

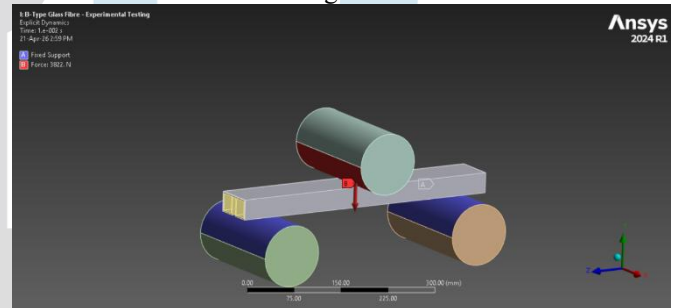


Fig - 33 Boundary conditions

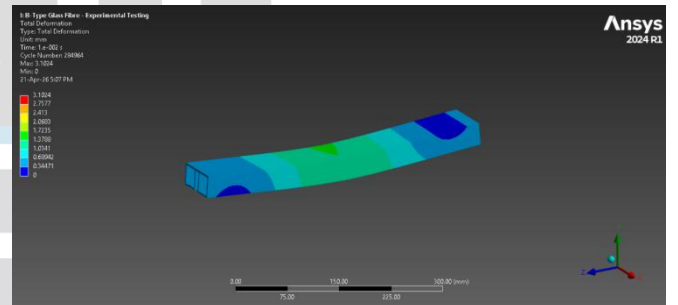


Fig - 34 Total deformation of the experimental prototype.

Total Deformation of the beam in ANSYS is around 3mm at the force of 3822 N.

The experimental setup and the Ansys results are nearly equal for the sample specimen. This proves that Ansys results are the nearly equal to the real-life results. So, the results of explicit dynamic results can be close to the real-life results.

Finite Element Analysis (FEA) was initially carried out on three different cross-sectional geometries of the side bumper beam, namely Hat-type, B-type, and rectangular sections, under identical loading and boundary conditions to identify the most suitable structural configuration.

For the Hat-type geometry, the maximum total deformation obtained was 61.361 mm, while the maximum directional deformation was 61.358 mm. The maximum equivalent (von Mises) stress reached 2746.3 MPa, and the structure generated a maximum reaction force of 9043.6 N. The total energy absorbed by this geometry during loading was 284.27 J.

For the B-type geometry, the maximum total deformation was 87.027 mm, and the maximum directional deformation was 86.94 mm. The equivalent stress developed in the beam reached 3095.6 MPa. However, this configuration demonstrated the

highest load-carrying capability among the three geometries with a maximum reaction force of 18738 N and a significantly higher energy absorption of 1409.5 J.

For the Rectangular geometry, the maximum total deformation recorded was 78.003 mm, with a directional deformation of 77.968 mm. The maximum equivalent stress was 690.73 MPa, which is comparatively lower than the other geometries. The maximum reaction force was 5244 N, and the total energy absorbed during impact was 339.77 J.

Based on these results, the B-type geometry demonstrated superior energy absorption and load resistance, indicating better crashworthiness performance. Therefore, this geometry was selected for further structural enhancement through composite reinforcement.

Subsequently, composite reinforcement was applied to the B-type geometry, and FEA was performed for Carbon Fiber Reinforced and E-Glass Fiber Reinforced bumper beams. For the Carbon Fiber Reinforced B-type beam, the maximum total deformation was 137.9 mm, while the maximum directional deformation was 91.446 mm. The equivalent stress developed reached 3437.2 MPa. This configuration produced a significantly high reaction force of 67401 N, with a total energy absorption capacity of 1728.1 J.

For the Glass Fiber Reinforced B-type beam, the maximum total deformation was 83.676 mm, and the directional deformation was 83.672 mm, which is considerably lower than that of the carbon fiber reinforced beam. The maximum equivalent stress observed was 3474.7 MPa. The beam developed a high reaction force of 54231 N and demonstrated the highest energy absorption capacity of 2197.7 J among all the configurations analyzed.

Comparatively, both composite reinforced beams significantly improved the structural performance of the bumper beam. However, the Glass Fiber Reinforced B-type beam showed a more balanced structural response with lower deformation and the highest energy absorption capability, making it more suitable for impact protection applications.

## 6. CONCLUSIONS

The present study focused on the design and strength optimization of a three-wheeler side bumper beam through comparative evaluation of different cross-sectional geometries and composite reinforcement using Finite Element Analysis.

The initial analysis revealed that the B-type cross-section offers superior crashworthiness characteristics, exhibiting the highest reaction force and energy absorption compared to Hat-type and rectangular sections. This indicates that the B-type geometry provides improved load distribution and better ability to manage impact energy.

To further enhance the structural performance and reduce weight, composite reinforcement was introduced to the B-type geometry using Epoxy Carbon UD and Glass Fiber materials. The analysis results show that both composite materials significantly improve the structural strength and impact energy absorption of the bumper beam. For the Epoxy Carbon UD reinforced beam energy absorption increased by 14 % and for the Glass Fiber reinforced beam energy absorption increased by 45%.

Among the two reinforced configurations, the Glass Fiber Reinforced B-type beam demonstrated the most favorable performance, with comparatively lower deformation and the highest energy absorption about 45% increased by conventional structural steel B type beam, while still maintaining high reaction force capability. The deformation is reduced by 12.35% in B type glass fiber reinforced beam than the conventional B type beam. This balanced combination of stiffness, strength, and energy absorption makes the glass fibre

reinforced configuration the most suitable design for side impact protection in three-wheelers.

Therefore, the Glass Fiber Reinforced B-type side bumper beam is observed as the optimized design from this study. By advancing material innovations, manufacturing techniques, and crashworthiness evaluations, bumper designs can be crucial in shaping the future of automotive safety and sustainability.

## ACKNOWLEDGEMENT

It gives me a great pleasure to present project on “Finite Element Analysis of 3-Wheeler Side Bumper Beam Using Composite Material” in partial fulfilment of requirement of Master of Engineering. I would like to express my gratitude to my project guide Dr.T.A. Jadhav who has invested his full effort in guiding me and whose contribution helped me to prepare this project. I am grateful to our respected HOD (Mechanical Dept.) Dr.A.P. Pandhare and Principal Dr.S.D. Lokhande, for providing all necessary facilities. Last but not the least, I would like to thank all the unseen authors of various articles on the internet for updating me about the latest technological aspects and for making me aware of the ongoing research in my seminar topic. I am also thankful to all my respected teachers and my colleague for their support

## REFERENCES:

- [1] Bennbaia, S.; Mahdi, E.; Abdella, G.; Dean, A. (2023) Composite Plastic Hybrid for Automotive Front Bumper Beam. *J. Compos. Sci.* 7, 162.
- [2] Du, B.; Li, Q.; Zheng, C.; Wang, S.; Gao, C.; Chen, L. (2023) Application of Lightweight Structure in Automobile Bumper Beam: A Review. *Materials* 16, 967.
- [3] Tshilidzi Valentia Mukhudwana; Wilson Webo; Moshibudi Caroline Khoathane; Brendon Mxolisi Shongwe: (2025) The Automotive Bumper Beam in the Era of the 4th Industrial Revolution: Review *The Journal of Engineering*; 2025:e70091
- [4] Vinjavarapu Sankararao, P. Nageswara Rao, Siva Sankara Babu, Medikonda Nageswararao, Kosaraju Satyanarayana; (2023) Enactment of Fiber Reinforced Hybrid Epoxy Composite for Passenger Car Bumper Beam; *E3S Web of Conferences* 391, 01171
- [5] Yeshanew, E. S., et al. (2023) Experimental investigation and crashworthiness analysis of automotive bumper beams. *Advances in Mechanical Engineering* Vol. 15(6) 1–23
- [6] Pai, A., Ayyoobi Kalliyath, S., Rodriguez-Millan, M., & Shenoy, S. B.; (2024) Crashworthiness analysis of filled/unfilled automotive bumper beams subjected to head-on collision events: a numerical approach. *Cogent engineering*, vol. 11, no. 1, 2399737
- [7] Ham, S.; Ji, S.; Cheon, S.S. (2024) The Design of a Piecewise-Integrated Composite Bumper Beam with Machine-Learning Algorithms. *Materials* 17, 602.
- [8] Rajpura, A., Prajapati, H., Sur, A., Jatti, V. S., Kale, G., & Razoumny, Y. (2025) Performance evaluation of lattice structured bumper beam for automobile. *Aims materials science*, 12(3): 395–422.
- [9] Prerit Tiwari, Bipul Kumar, Pransh Khanna, Baskar Ponnusamy: (2025) Engineering an Ultra-Light Bumper for Passenger Vehicles. *International Research Journal of Multidisciplinary Scope (IRJMS)*; 6(2): 1428-1442
- [10] Wagh, J. P., & Kulkarni, S. D.; (2024) Investigative studies on natural fiber reinforced composites for automotive bumper beam applications: A review.: *Journal of Reinforced Plastics and Composites*, Vol. 0(0) 1–11
- [11] B.G.; Padmanabhan, S.; Gautam, D.; Khan, F.; Baskar, S.; Saravanan, A.L.; Sharma, A. (2024) An Investigation into the Design and Analysis of the Front Frame Bumper with Dynamic Load Impact. *Eng. Proc.* 2024, 66, 6
- [12] Chawla, K., Ahmed Arabi Hassena, Nikhil Garga, Deepak Kumar Pokkallaa; (2025) Property Optimized Energy

Absorber for Automotive Bumper Using Lattice Structures and Multi-Materials: *Materials & Design* 253 113724

- [13] Wu, B.; Chen, Q.; Liu, F.; Chen, M.; Lu, Y.; Jiang, D.; Yi, Y. (2023) Study on Dynamic Mechanics of Node-Enhanced Graded Lattice Structure and Application Optimization in Automobile Energy Absorbing Box. *Materials*, 16, 6893
- [14] Yalçın, M.M. (2024) Flexural Behavior of 3D-Printed Carbon Fiber-Reinforced Nylon Lattice Beams. *Polymers*, 16, 2991
- [15] Sliwa, A., Mikołajko, W., Bonek, M., & Dziwis, A.; (2024) Strength Analysis of the Front Bumper Beam of a Passenger Car: *Arch. Metall. Mater.* 69, 2, 711-716

